IOP Conf. Series: Materials Science and Engineering **378** (2018) 012017 doi:10.1088/1757-899X/378/1/012017

Dynamic Characteristics Analysis of Spiral Groove Liquid Lubricated Seal Considering Centrifugal Inertia

W J Yang, M M Hao, Z T Li and H C Cao

College of Chemical Engineering, China University of Petroleum (East China), Qingdao, 266580, China

E-mail: yangwen516@126.com

Abstract. A three degree of freedom model of spiral groove liquid lubricated seal was established for studying the effects of centrifugal inertia on dynamic characteristics. The dynamic stiffness and damping coefficients of liquid lubricated seal with centrifugal inertia and those without centrifugal inertia were obtained by means of finite element method, and then comparative analysis was carried out. Results indicate that dynamic stiffness and damping coefficients are increased linearly with the increase of rotating speed. Dynamic stiffness and damping coefficients decrease with the increasing film thickness. The effects of centrifugal inertia on axial stiffness coefficient and angular coupling stiffness coefficient can be neglected under different rotating speed and different film thickness. When the values of rotating speed and film thickness are large, the effect of centrifugal inertia on angle stiffness coefficient cannot be ignored. Centrifugal inertia has no effects on dynamic damping coefficients with the variation of rotating speed and film thickness.

1. Introduction

The spiral groove liquid lubricated mechanical seal has been widely applied in the field of rotary machinery, such as pumps, compressors, mixers and so on. Its configuration is shown in figure 1. Compared with a conventional mechanical seal, the surface of rotating ring contains a pattern of shallow spiral grooves, which generate the hydrodynamic pressure to separate the sealing rings [1]. With the increasing rotating speed, a great deal of work has been done on centrifugal inertia. However, most of the work has dealt with bearings [2-3]. The Reynolds equation incorporating centrifugal forces was derived by Pinkus and Lund [4], and then an analysis was conducted and solutions were provided for the effect of centrifugal forces on the hydrodynamics of high-speed thrust bearings and seals. Gupta and Sharma presented the analysis of centrifugal inertia effects in fluid-film-lubricated misaligned radial face seals [5]. Nowadays, most researchers have neglected the centrifugal inertia but Zhao did some work on spiral-groove rotary seal ring with considering the effect of centrifugation [6-7]. The ability to eliminate or minimize direct face contact during runtime is the key to the success of a liquid lubricated face seal. If the stator cannot track the rotor properly, seal face contact may occur, which would lead to face wear or seal failure [8]. Thus, it is important to study the effect of centrifugal inertia on dynamic characteristics of liquid lubricated seals.

In this paper, a three degree of freedom model of spiral groove liquid lubricated seal is established. The stiffness and damping coefficients of liquid lubricated seal with centrifugal inertia and those without centrifugal inertia are obtained by the perturbation method and the finite element method. Then comparative analysis is carried out. The results can provide theoretical guidance for the design and application of liquid lubricated seal under different operating conditions.

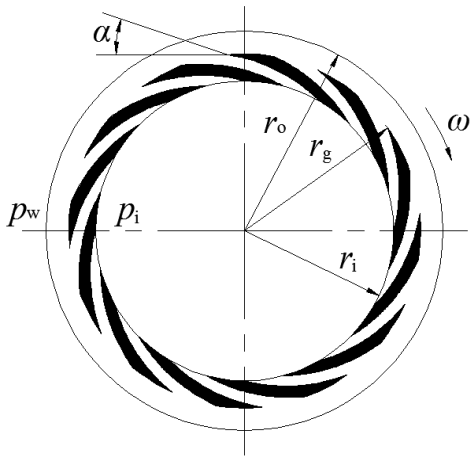

Figure 1. Geometry schematic diagram of rotating ring.

The following analysis is based on the parameters listed in table 1, which includes seal geometry and operating conditions.

Table 1. Parameters for the analysis of a spiral groove liquid lubricated seal

Parameters	Working conditions
inner radius r_i(m)	0.04425
outer radius r_o(m)	0.05325
spiral groove radius r_g(m)	0.05055
spiral groove depth h_g(m)	12.5×10^{-6}
spiral groove angle α(°)	18
spiral groove number N_g	12
land-to-groove ratio	1
lubricant velocity μ(Pa s)	0.001003
lubricant temperature (℃)	25
lubricant density ρ(kg m^{-3})	1000
inner pressure p_i(MPa)	0.6
outer pressure p_w(MPa)	0.4

2. Governing equations

To establish the mathematical model, some basic assumptions are made as following.

- The fluid between the sealing faces can be characterized as Newtonian fluid, and it is isothermal and isoviscous. Also, the fluid film is laminar.
- The seal face is smooth and no face contact happens in the operation.

The Reynolds equation considering centrifugal inertia can be expressed in the dimension form as follows [9]:

$$\frac{\partial}{\partial r}\left[\frac{r\rho h^3}{\mu}\left(\frac{\partial p}{\partial r}\right)\right]+\frac{1}{r}\frac{\partial}{\partial\theta}\left[\frac{\rho h^3}{\mu}\left(\frac{\partial p}{\partial\theta}\right)\right]=6r\omega\frac{\partial(\rho h)}{\partial\theta}+12r\frac{\partial(\rho h)}{\partial t}+\frac{3\omega^2}{10\mu}\frac{\partial\left(\rho^2r^2h^3\right)}{\partial r} \tag{1}$$

When the seal is perturbed by a small oscillatory motion (Δz, $\Delta\gamma_x$, $\Delta\gamma_y$) with frequency f, according to the kinematics shown in figure 2, the seal displacement can be expressed as the following:

$$h=h_0+\Delta z+r\sin\theta\Delta\gamma_x-r\cos\theta\Delta\gamma_y \tag{2}$$

where $\Delta z=|\Delta z|e^{ift}$, $\Delta\gamma_x=|\Delta\gamma_x|e^{ift}$, $\Delta\gamma_y=|\Delta\gamma_y|e^{ift}$. h_0 is the steady-state equilibrium film thickness.

These small motions cause a small pressure perturbation about the equilibrium pressure p_0, and then the total pressure can be expressed as

$$p = p_0 + p_z\Delta z + p_x\Delta\gamma_x + p_y\Delta\gamma_y \tag{3}$$

Because the motions are defined in complex form, the corresponding perturbation pressures are also complexes, which can be written as

$$p_z = p_{zr} + \mathrm{i}p_{zi}\,,\ \ p_x = p_{xr} + \mathrm{i}p_{xi}\,,\ \ p_y = p_{yr} + \mathrm{i}p_{yi} \tag{4}$$

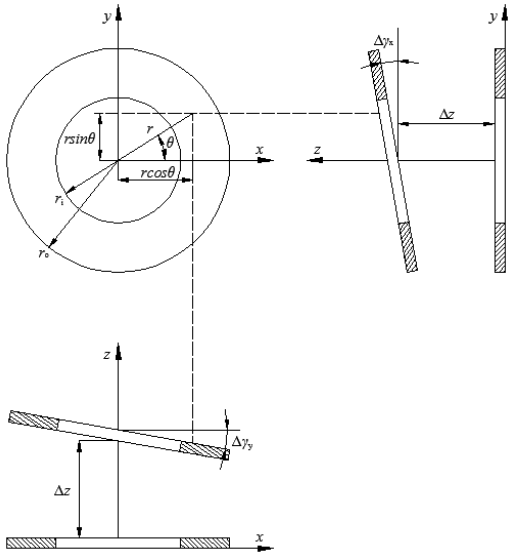

Figure 2. Seal perturbation model andcoordinate system.

Substituting relationships from equation (2) to equation (4) into equation (1) and neglecting higher order terms yields the following seven dimensionless equations:

$$\frac{\partial}{R\partial R}\left(RH^3\frac{\partial\overline{P}}{\partial R}\right)+\frac{1}{R^2}\frac{\partial}{\partial\theta}\left(H^3\frac{\partial\overline{P}}{\partial\theta}\right)=K_1\frac{\partial H}{\partial\theta}+K_2\frac{\partial\left(R^2H^3\right)}{R\partial R} \tag{5}$$

$$\frac{\partial}{R\partial R}\left(RH^3\frac{\partial\overline{P}_{zr}}{\partial R}\right)+\frac{\partial}{R\partial R}\left(3RH^2\frac{\partial\overline{P}}{\partial R}\right)+\frac{1}{R^2}\frac{\partial}{\partial\theta}\left(H^3\frac{\partial\overline{P}_{zr}}{\partial\theta}\right)+\frac{1}{R^2}\frac{\partial}{\partial\theta}\left(3H^2\frac{\partial\overline{P}}{\partial\theta}\right)=K_2\frac{\partial\left(3R^2H^2\right)}{R\partial R} \tag{6a}$$

$$\frac{\partial}{R\partial R}\left(RH^3\frac{\partial\overline{P}_{zi}}{\partial R}\right)+\frac{1}{R^2}\frac{\partial}{\partial\theta}\left(H^3\frac{\partial\overline{P}_{zi}}{\partial\theta}\right)=2K_1\omega_1 \tag{6b}$$

$$\begin{aligned}&\frac{\partial}{R\partial R}\left(RH^3\frac{\partial\overline{P}_{xr}}{\partial R}\right)+\frac{\partial}{R\partial R}\left(3H^2R^2\sin\theta\frac{\partial\overline{P}}{\partial R}\right)+\frac{1}{R^2}\frac{\partial}{\partial\theta}\left(H^3\frac{\partial\overline{P}_{xr}}{\partial\theta}\right)+\frac{1}{R^2}\frac{\partial}{\partial\theta}\left(3H^2R\sin\theta\frac{\partial\overline{P}}{\partial\theta}\right)\\&=K_1\frac{\partial\left(R\sin\theta\right)}{\partial\theta}+K_2\frac{\partial}{R\partial R}\left(3H^2R^3\sin\theta\right)\end{aligned} \tag{7a}$$

$$\frac{\partial}{R\partial R}\left(RH^3\frac{\partial\overline{P}_{xi}}{\partial R}\right)+\frac{1}{R^2}\frac{\partial}{\partial\theta}\left(H^3\frac{\partial\overline{P}_{xi}}{\partial\theta}\right)=2K_1\omega_1R\sin\theta \tag{7b}$$

$$\frac{\partial}{R\partial R}\left(RH^3\frac{\partial \overline{P}_{\mathrm{yr}}}{\partial R}\right)+\frac{\partial}{R\partial R}\left(-3H^2R^2\cos\theta\frac{\partial \overline{P}}{\partial R}\right)+\frac{1}{R}\frac{\partial}{\partial\theta}\left(\frac{H^3}{R}\frac{\partial \overline{P}_{\mathrm{yr}}}{\partial\theta}\right)+\frac{1}{R}\frac{\partial}{\partial\theta}\left(-3H^2\cos\theta\frac{\partial \overline{P}}{\partial\theta}\right)$$
$$=-K_1\frac{\partial(R\cos\theta)}{\partial\theta}-K_2\frac{\partial}{R\partial R}\left(3H^2R^3\cos\theta\right) \tag{8a}$$

$$\frac{\partial}{R\partial R}\left(RH^3\frac{\partial \overline{P}_{\mathrm{yi}}}{\partial R}\right)+\frac{1}{R^2}\frac{\partial}{\partial\theta}\left(H^3\frac{\partial \overline{P}_{\mathrm{yi}}}{\partial\theta}\right)=-2K_1\omega_1R\cos\theta \tag{8b}$$

where $R=\frac{r}{r_{\mathrm{o}}}$, $\overline{P}=\frac{p_0}{p_{\mathrm{w}}}$, $H=\frac{h_0}{h_{\mathrm{i}}}$, $\omega_1=\frac{f}{\omega}$, $\overline{P}_{\mathrm{zr}}=\frac{p_{\mathrm{zr}}h_{\mathrm{i}}}{p_{\mathrm{w}}}$, $\overline{P}_{\mathrm{zi}}=\frac{p_{\mathrm{zi}}h_{\mathrm{i}}}{p_{\mathrm{w}}}$, $\overline{P}_{\mathrm{xr}}=\frac{p_{\mathrm{xr}}h_{\mathrm{i}}}{p_{\mathrm{w}}r_{\mathrm{o}}}$, $\overline{P}_{\mathrm{xi}}=\frac{p_{\mathrm{xi}}h_{\mathrm{i}}}{p_{\mathrm{w}}r_{\mathrm{o}}}$, $\overline{P}_{\mathrm{yr}}=\frac{p_{\mathrm{yr}}h_{\mathrm{i}}}{p_{\mathrm{w}}r_{\mathrm{o}}}$, $\overline{P}_{\mathrm{yi}}=\frac{p_{\mathrm{yi}}h_{\mathrm{i}}}{p_{\mathrm{w}}r_{\mathrm{o}}}$, $K_1=\frac{6\mu\omega r_{\mathrm{o}}^2}{p_{\mathrm{w}}h_{\mathrm{i}}^2}$, $K_2=\frac{3\rho\omega^2r_{\mathrm{o}}^2}{10p_{\mathrm{w}}}$. ω is the rotating speed. h_{i} is the film thickness. When K_2 equals 0, equations from equation (5) to equation (8b) are the steady and dynamic Reynolds equations without considering centrifugal inertia.

The following boundary conditions are used to solve the equations.

$$\overline{P}=\overline{P}_{\mathrm{i}}=p_{\mathrm{i}}/p_{\mathrm{w}} \text{ at } R=R_{\mathrm{i}}=r_{\mathrm{i}}/r_{\mathrm{o}},$$

$$\overline{P}=\overline{P}_{\mathrm{w}}=1 \text{ at } R=R_{\mathrm{o}}=1,$$

$$\overline{P}(\theta,R)=\overline{P}(\theta+2\pi,R),$$

$$\overline{P}_{\mathrm{zr}}=\overline{P}_{\mathrm{zi}}=\overline{P}_{\mathrm{xr}}=\overline{P}_{\mathrm{xi}}=\overline{P}_{\mathrm{yr}}=\overline{P}_{\mathrm{yi}}=0 \text{ at } R=r_{\mathrm{i}}/r_{\mathrm{o}} \text{ and } R=1.$$

Equation (5) is a linear equation that governs the steady-state pressure distribution at the equilibrium position. The solution is obtained by a Galerkin finite element method, and then it is used as the input to solve the remaining equations.

The perturbation pressure Δp is viewed as a function of perturbation displacement and perturbation velocity of the static ring. Using a first order Taylor series expansion, the perturbation pressure can be expressed as

$$\Delta p=p_{\mathrm{zz}}\Delta z+p_{\mathrm{xx}}\Delta\gamma_{\mathrm{x}}+p_{\mathrm{yy}}\Delta\gamma_{\mathrm{y}}+p_{\dot{\mathrm{z}}}\Delta\dot{z}+p_{\dot{\mathrm{x}}}\Delta\dot{\gamma}_{\mathrm{x}}+p_{\dot{\mathrm{y}}}\Delta\dot{\gamma}_{\mathrm{y}} \tag{9}$$

The axial force and angular moments in response to the perturbation pressure can be expressed in the following form

$$\begin{Bmatrix}\mathrm{d}F_{\mathrm{z}}\\ \mathrm{d}M_{\mathrm{x}}\\ \mathrm{d}M_{\mathrm{y}}\end{Bmatrix}=\iint_A\begin{Bmatrix}1\\ r\sin\theta\\ -r\cos\theta\end{Bmatrix}\Delta p\mathrm{d}A=\iint_A\begin{Bmatrix}1\\ r\sin\theta\\ -r\cos\theta\end{Bmatrix}\left(p_{\mathrm{zz}}\Delta z+p_{\mathrm{xx}}\Delta\gamma_{\mathrm{x}}+p_{\mathrm{yy}}\Delta\gamma_{\mathrm{y}}+p_{\dot{\mathrm{z}}}\Delta\dot{z}+p_{\dot{\mathrm{x}}}\Delta\dot{\gamma}_{\mathrm{x}}+p_{\dot{\mathrm{y}}}\Delta\dot{\gamma}_{\mathrm{y}}\right)dA$$
$$=\iint_A\begin{Bmatrix}1\\ r\sin\theta\\ -r\cos\theta\end{Bmatrix}\left[\left(p_{\mathrm{zz}}+\mathrm{i}fp_{\dot{\mathrm{z}}}\right)|\Delta z|\mathrm{e}^{\mathrm{i}ft}+\left(p_{\mathrm{xx}}+\mathrm{i}fp_{\dot{\mathrm{x}}}\right)|\Delta\gamma_{\mathrm{x}}|\mathrm{e}^{\mathrm{i}ft}+\left(p_{\mathrm{yy}}+\mathrm{i}fp_{\dot{\mathrm{y}}}\right)|\Delta\gamma_{\mathrm{y}}|\mathrm{e}^{\mathrm{i}ft}\right]\mathrm{d}A \tag{10}$$
$$=\iint_A\begin{bmatrix}p_{\mathrm{zz}} & p_{\mathrm{xx}} & p_{\mathrm{yy}}\\ r\sin\theta p_{\mathrm{zz}} & r\sin\theta p_{\mathrm{xx}} & r\sin\theta p_{\mathrm{yy}}\\ -r\cos\theta p_{\mathrm{zz}} & -r\cos\theta p_{\mathrm{xx}} & -r\cos\theta p_{\mathrm{yy}}\end{bmatrix}\mathrm{d}A\begin{Bmatrix}\Delta z\\ \Delta\gamma_{\mathrm{x}}\\ \Delta\gamma_{\mathrm{y}}\end{Bmatrix}+\iint_A\begin{bmatrix}p_{\dot{\mathrm{z}}} & p_{\dot{\mathrm{x}}} & p_{\dot{\mathrm{y}}}\\ r\sin\theta p_{\dot{\mathrm{z}}} & r\sin\theta p_{\dot{\mathrm{x}}} & r\sin\theta p_{\dot{\mathrm{y}}}\\ -r\cos\theta p_{\dot{\mathrm{z}}} & -r\cos\theta p_{\dot{\mathrm{x}}} & -r\cos\theta p_{\dot{\mathrm{y}}}\end{bmatrix}\mathrm{d}A\times\begin{Bmatrix}\Delta\dot{z}\\ \Delta\dot{\gamma}_{\mathrm{x}}\\ \Delta\dot{\gamma}_{\mathrm{y}}\end{Bmatrix}$$

Compared with equation (4), the real parts and imaginary parts of perturbation pressures can be expressed as

$$p_{\mathrm{zr}}=p_{\mathrm{zz}},\ p_{\mathrm{zi}}=fp_{\dot{\mathrm{z}}},\ p_{\mathrm{xr}}=p_{\mathrm{xx}},\ p_{\mathrm{xi}}=fp_{\dot{\mathrm{x}}},$$

$$p_{\mathrm{yr}}=p_{\mathrm{yy}},\ p_{\mathrm{yi}}=fp_{\dot{\mathrm{y}}}.$$

Introducing the following form

$$\begin{Bmatrix} \mathrm{d}F_{\mathrm{z}} \\ \mathrm{d}M_{\mathrm{x}} \\ \mathrm{d}M_{\mathrm{y}} \end{Bmatrix} = -\begin{bmatrix} k_{\mathrm{zz}} & k_{\mathrm{zx}} & k_{\mathrm{zy}} \\ k_{\mathrm{xz}} & k_{\mathrm{xx}} & k_{\mathrm{xy}} \\ k_{\mathrm{yz}} & k_{\mathrm{yx}} & k_{\mathrm{yy}} \end{bmatrix} \times \begin{Bmatrix} \Delta z \\ \Delta\gamma_{\mathrm{x}} \\ \Delta\gamma_{\mathrm{y}} \end{Bmatrix} - \begin{bmatrix} c_{\mathrm{zz}} & c_{\mathrm{zx}} & c_{\mathrm{zy}} \\ c_{\mathrm{xz}} & c_{\mathrm{xx}} & c_{\mathrm{xy}} \\ c_{\mathrm{yz}} & c_{\mathrm{yx}} & c_{\mathrm{yy}} \end{bmatrix} \times \begin{Bmatrix} \Delta\dot{z} \\ \Delta\dot{\gamma}_{\mathrm{x}} \\ \Delta\dot{\gamma}_{\mathrm{y}} \end{Bmatrix} \tag{11}$$

Comparing equation (10) with equation (11), the dimensionless stiffness and damping coefficients are easily identified

$$\begin{bmatrix} K_{\mathrm{zz}} & K_{\mathrm{zx}} & K_{\mathrm{zy}} \\ K_{\mathrm{xz}} & K_{\mathrm{xx}} & K_{\mathrm{xy}} \\ K_{\mathrm{yz}} & K_{\mathrm{yx}} & K_{\mathrm{yy}} \end{bmatrix} = -\iint_A \begin{bmatrix} \overline{P}_{\mathrm{zr}} & \overline{P}_{\mathrm{xr}} & \overline{P}_{\mathrm{yr}} \\ R\sin\theta\overline{P}_{\mathrm{zr}} & R\sin\theta\overline{P}_{\mathrm{xr}} & R\sin\theta\overline{P}_{\mathrm{yr}} \\ -R\cos\theta\overline{P}_{\mathrm{zr}} & -R\cos\theta\overline{P}_{\mathrm{xr}} & -R\cos\theta\overline{P}_{\mathrm{yr}} \end{bmatrix} \mathrm{d}A \tag{12}$$

$$\begin{bmatrix} C_{\mathrm{zz}} & C_{\mathrm{zx}} & C_{\mathrm{zy}} \\ C_{\mathrm{xz}} & C_{\mathrm{xx}} & C_{\mathrm{xy}} \\ C_{\mathrm{yz}} & C_{\mathrm{yx}} & C_{\mathrm{yy}} \end{bmatrix} = -\frac{1}{\omega_1}\iint_A \begin{bmatrix} \overline{P}_{\mathrm{zi}} & \overline{P}_{\mathrm{xi}} & \overline{P}_{\mathrm{yi}} \\ R\sin\theta\overline{P}_{\mathrm{zi}} & R\sin\theta\overline{P}_{\mathrm{xi}} & R\sin\theta\overline{P}_{\mathrm{yi}} \\ -R\cos\theta\overline{P}_{\mathrm{zi}} & -R\cos\theta\overline{P}_{\mathrm{xi}} & -R\cos\theta\overline{P}_{\mathrm{yi}} \end{bmatrix} \mathrm{d}A \tag{13}$$

where $K_{\mathrm{zz}}=\frac{k_{\mathrm{zz}}h_{\mathrm{i}}}{p_{\mathrm{w}}r_{\mathrm{o}}^2}$, $K_{\mathrm{zx}}=\frac{k_{\mathrm{zx}}h_{\mathrm{i}}}{p_{\mathrm{w}}r_{\mathrm{o}}^3}$, $K_{\mathrm{zy}}=\frac{k_{\mathrm{zy}}h_{\mathrm{i}}}{p_{\mathrm{w}}r_{\mathrm{o}}^3}$, $K_{\mathrm{xz}}=\frac{k_{\mathrm{xz}}h_{\mathrm{i}}}{p_{\mathrm{w}}r_{\mathrm{o}}^3}$, $K_{\mathrm{xx}}=\frac{k_{\mathrm{xx}}h_{\mathrm{i}}}{p_{\mathrm{w}}r_{\mathrm{o}}^4}$, $K_{\mathrm{xy}}=\frac{k_{\mathrm{xy}}h_{\mathrm{i}}}{p_{\mathrm{w}}r_{\mathrm{o}}^4}$, $K_{\mathrm{yz}}=\frac{k_{\mathrm{yz}}h_{\mathrm{i}}}{p_{\mathrm{w}}r_{\mathrm{o}}^3}$, $K_{\mathrm{yx}}=\frac{k_{\mathrm{yx}}h_{\mathrm{i}}}{p_{\mathrm{w}}r_{\mathrm{o}}^4}$, $K_{\mathrm{yy}}=\frac{k_{\mathrm{yy}}h_{\mathrm{i}}}{p_{\mathrm{w}}r_{\mathrm{o}}^4}$, $C_{\mathrm{zz}}=\frac{c_{\mathrm{zz}}h_{\mathrm{i}}\omega}{p_{\mathrm{w}}r_{\mathrm{o}}^2}$, $C_{\mathrm{zx}}=\frac{c_{\mathrm{zx}}h_{\mathrm{i}}\omega}{p_{\mathrm{w}}r_{\mathrm{o}}^3}$, $C_{\mathrm{zy}}=\frac{c_{\mathrm{zy}}h_{\mathrm{i}}\omega}{p_{\mathrm{w}}r_{\mathrm{o}}^3}$, $C_{\mathrm{xz}}=\frac{c_{\mathrm{xz}}h_{\mathrm{i}}\omega}{p_{\mathrm{w}}r_{\mathrm{o}}^3}$, $C_{\mathrm{xx}}=\frac{c_{\mathrm{xx}}h_{\mathrm{i}}\omega}{p_{\mathrm{w}}r_{\mathrm{o}}^4}$, $C_{\mathrm{xy}}=\frac{c_{\mathrm{xy}}h_{\mathrm{i}}\omega}{p_{\mathrm{w}}r_{\mathrm{o}}^4}$, $C_{\mathrm{yz}}=\frac{c_{\mathrm{yz}}h_{\mathrm{i}}\omega}{p_{\mathrm{w}}r_{\mathrm{o}}^3}$, $C_{\mathrm{yx}}=\frac{c_{\mathrm{yx}}h_{\mathrm{i}}\omega}{p_{\mathrm{w}}r_{\mathrm{o}}^4}$, $C_{\mathrm{yy}}=\frac{c_{\mathrm{yy}}h_{\mathrm{i}}\omega}{p_{\mathrm{w}}r_{\mathrm{o}}^4}$.

3. Results and discussion

The calculation results show that angular coupling stiffness coefficients K_{zx}, K_{zy}, K_{xz}, K_{yz} and angular coupling damping coefficients C_{zx}, C_{zy}, C_{xz}, C_{yz} are all equal to zero. Angular stiffness coefficients $K_{\mathrm{xx}}=K_{\mathrm{yy}}$, $K_{\mathrm{xy}}=-K_{\mathrm{yx}}$. Angular damping coefficients $C_{\mathrm{xx}}=C_{\mathrm{yy}}$, $C_{\mathrm{xy}}=C_{\mathrm{yx}}=0$.

3.1. Effects of centrifugal inertia under different rotating speed

Figure 3 shows the effects of centrifugal inertia on dynamic stiffness coefficients under different rotating speed. It can be seen that the dynamic stiffness coefficients increase linearly with the increase of rotating speed. The effect of rotating speed on axial stiffness coefficient K_{zz} is greater than that on angular stiffness coefficient K_{xx} (K_{yy}). However, the effect of rotating speed on angular coupling stiffness coefficient K_{xy} ($-K_{\mathrm{yx}}$) is the smallest. At the same time, it can be found that the dynamic stiffness coefficients with centrifugal inertia are basically the same as those without centrifugal inertia. The relative errors increase linearly with the increase of rotating speed. When the rotating speed is 12000 r·min^{-1}, the relative error is respectively 0.68%, 0.81% and 0.19%, which can be neglected.

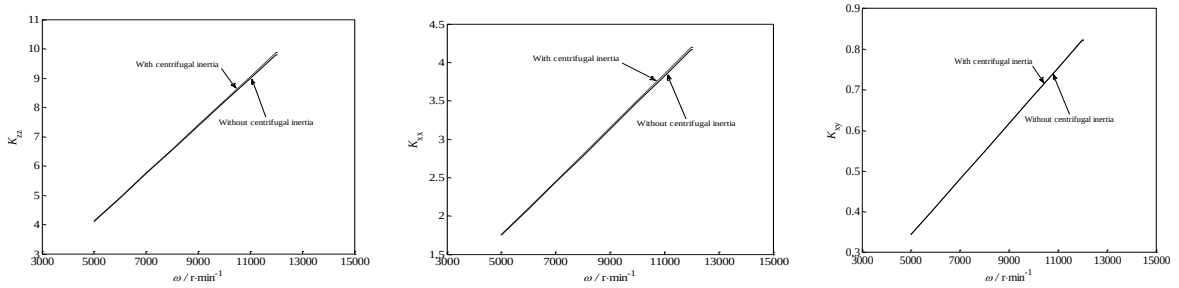

(a) (b) (c)

Figure 3. Effects of centrifugal inertia on dynamic stiffness coefficients under different rotating speed.

Figure 4 describes the effects of centrifugal inertia on dynamic damping coefficients under different rotating speed. The figures show that the dynamic damping coefficients increase with the increase of rotating speed, which is basically linear. The effect of rotating speed on axial damping coefficient C_{zz} is greater than that on angular damping coefficient C_{xx} (C_{yy}). Compared the dynamic damping coefficients with centrifugal inertia and those without centrifugal inertia under the same rotating speed, it is known that the two are exactly the same, so centrifugal inertia has no effect on dynamic damping coefficients when rotating speed changes.

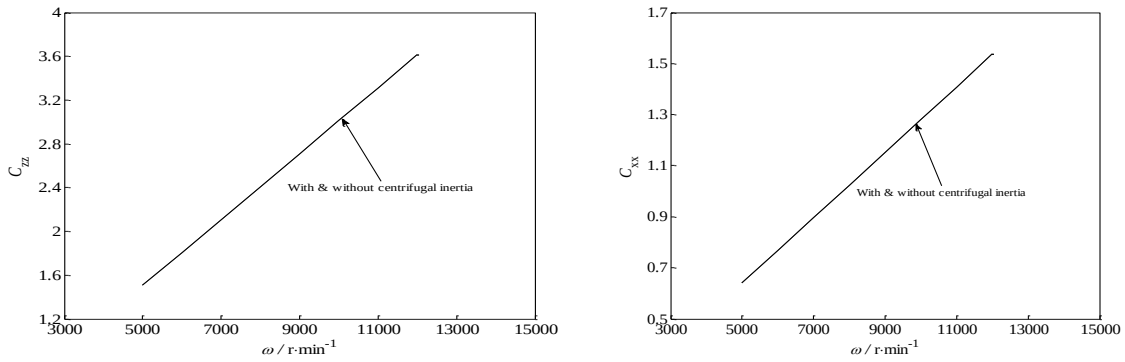

(a) (b)

Figure 4. Effects of centrifugal inertia on dynamic damping coefficients under different rotating speed.

3.2. Effects of centrifugal inertia under different film thickness

Figure 5 shows the effects of centrifugal inertia on dynamic stiffness coefficients under different film thickness. From the figures, we know that axial stiffness coefficient K_{zz} and angular stiffness coefficient K_{xx} (K_{yy}) decrease rapidly with the increase of film thickness firstly, and then the trend of decline is slow and tends to zero. Besides, the change of K_{zz} is more significant than that of K_{xx} (K_{yy}). The angular coupling stiffness coefficient K_{xy} ($-K_{yx}$) decreases gradually and tends to zero as the film thickness increases. Compared the dynamic stiffness coefficients with centrifugal inertia and those without centrifugal inertia, we can know that the relative errors increase as the film thickness increases, and the relative error is respectively 3.26%、5.08% and 0.26% when the film thickness is about 15×10^{-6} m.

Figure 6 gives the effects of centrifugal inertia on dynamic damping coefficients under different film thickness. The figures show that axial damping coefficient C_{zz} and angular damping coefficient C_{xx} (C_{yy}) are decreased rapidly with the increase of film thickness and the change of C_{zz} is more obvious. With a further increase of film thickness, axial damping coefficient and angular damping coefficient decrease slowly and tend to zero. The dynamic damping coefficients with centrifugal inertia are exactly the same as those without centrifugal inertia under the same film thickness. Therefore, centrifugal inertia has no effect on dynamic damping coefficients when film thickness changes.

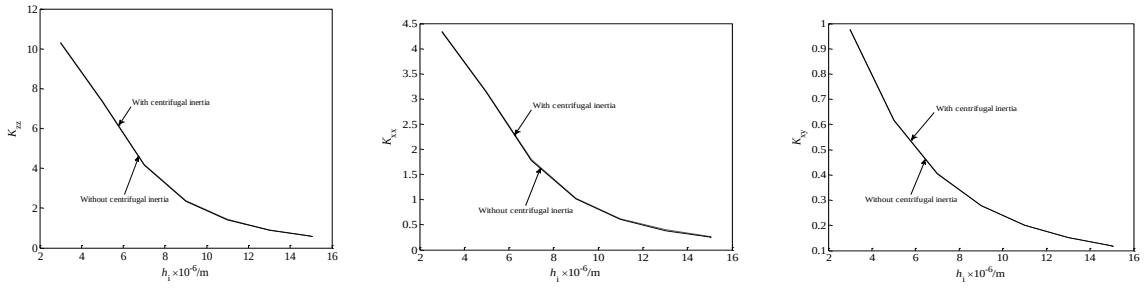

(a) (b) (c)

Figure 5. Effects of centrifugal inertia on dynamic stiffness coefficients under different film thickness.

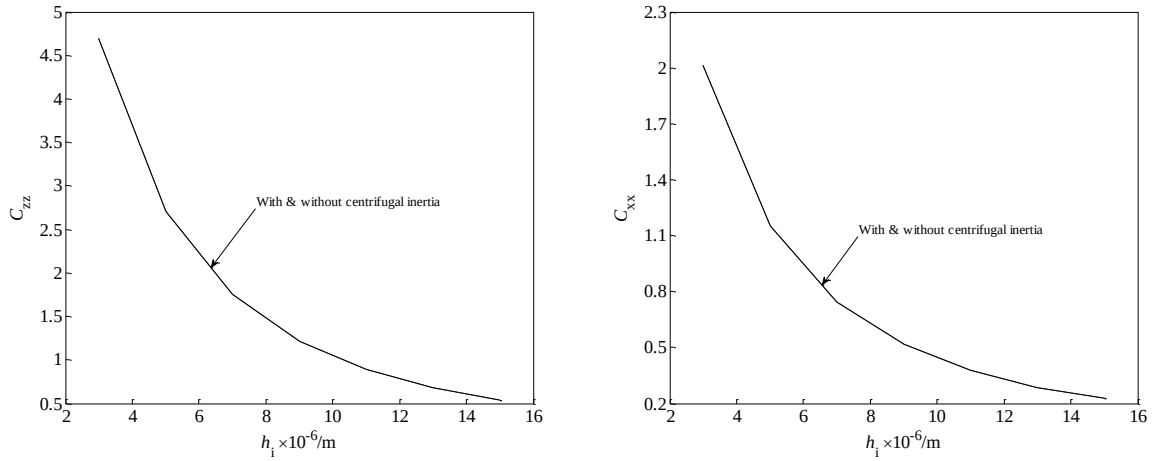

Figure 6. Effects of centrifugal inertia on dynamic damping coefficients under different film thickness.

4. Conclusions

In this paper, the stiffness and damping coefficients are obtained by solving the dynamic Reynolds equation using the perturbation technique. Results show that the effects of centrifugal inertia on axial stiffness coefficient and angular coupling stiffness coefficient can be neglected under different rotating speed and different film thickness. When the values of rotating speed and film thickness are large, the effect of centrifugal inertia on angle stiffness coefficient cannot be ignored. Centrifugal inertia has no effects on dynamic damping coefficients with the variation of rotating speed and film thickness.

It should be noted that the fluid pressure in this work is greater than cavitation pressure, and a cavitation phenomenon doesn't takes place. However, when the film thickness is small or the fluid is oil, the fluid pressure may be less than cavitation pressure, which should be studied in the future.

5. Acknowledgment

The authors gratefully acknowledge the financial support by the National Natural Science Foundation of China (51375497), and the Graduate Innovation Project of China University of Petroleum (East China) (YCXJ2016040).

6. References

[1] Salant R F and Homiller S J 1993 Stiffness and leakage in spiral groove upstream pumping mechanical seals. *Tribology Transactions*, **36** 55-60.

[2] Kakoty S K and Majumdar B C 1999 Effect of fluid inertia on stability of flexibly supported oil journal bearings: linear perturbation analysis. *Tribology International*, **32** 217-28.

[3] Nassab G S A 2005 Inertia effect on the thermohydrodynamic characteristics of journal bearings. *Proceedings of the Institution of Mechanical Engineers, Part J: Journal of Engineering Tribology*, **219** 459-67.

[4] Pinkus O and Lund J W 1981 Centrifugal effects in thrust bearings and seals under laminar conditions. *ASME Journal of Lubrication Technology*, **103** 126-36.

[5] Gupta R S and Sharma L G 1989 Centrifugal inertia effects in misaligned radial face seals. *Wear*, **129** 319-32.

[6] Zhao Y M, Hu J B and Wei C 2014 Dynamic analysis of spiral-groove rotary seal ring for wet clutches. *Journal of Tribology*, **136** 0317101-10.

[7] Zhao Y M, Yuan S H, Hu J B and Wei C 2015 Nonlinear dynamic analysis of rotary seal ring considering creep rotation. *Tribology International*, **82** 101-09.

[8] Ruan B 2002 A semi-analytical solution to the dynamic tracking of non-contacting gas face seals. *Journal of Tribology*, **124** 196-202.
[9] HimYu T and Sadeghi F 2001 Groove effects on thrust washer lubrication. *Journal of Tribology*, **123** 295-304.